Probing the Structure of the Nicotinic Acetylcholine Receptor with the Hydrophobic Photoreactive Probes [^{125}I]TID-BE and [^{125}I]TIDPC/16[†]

Michael P. Blanton,* Elizabeth A. McCardy, Angela Huggins, and Dipen Parikh

Department of Pharmacology, Texas Tech University Health Sciences Center, 3601 Fourth Street, Lubbock, Texas 79430

Received June 17, 1998; Revised Manuscript Received August 4, 1998

ABSTRACT: The hydrophobic photoreactive compound 3-trifluoromethyl-3-(*m*-[^{125}I]iodophenyl) diazirine ([^{125}I]TID) has revealed important structural information about the pore of the ion channel and lipid−protein interface of the nicotinic acetylcholine receptor (AChR). To further characterize the structure of the AChR, we have mapped the sites of photoincorporation of a benzoic acid ester analogue of TID ([^{125}I]TID-BE) and a phospholipid analogue ([^{125}I]TIDPC/16). For each photoreactive probe, labeled sites were identified by amino-terminal sequencing of purified tryptic fragments of individual receptor subunits. [^{125}I]TID-BE reacted with αCys-412, αMet-415, and αCys-418 in the M4 segment of the α-subunit and γCys-451 and γSer-460 in γM4. In the M1 segment of the α- and β-subunits, [^{125}I]TID-BE labeled αPhe-227, αLeu-228, and βLeu-234, βAla-235, respectively. The labeling pattern in the M1 and M4 segments indicate that TID and TID-BE interact with the AChR lipid−protein interface in a similar fashion, revealing the same lipid-exposed face of each transmembrane segment. In contrast to TID, there was, however, no detectable incorporation of [^{125}I]TID-BE into the channel lining βM2 segment when the AChR was labeled in the resting state conformation. In the presence of agonist (desensitized state), [^{125}I]TID-BE reacted with βLeu-257, βVal-261, and β-Leu-264 in βM2; a labeling pattern which indicates that, in comparison to TID, the binding loci for TID-BE is located closer to the extracellular end of the channel. For [^{125}I]TIDPC/16, receptor labeling was insensitive to the presence of agonist and the sites of incorporation mapped to the confines of the transmembrane segments αM4, αM1, and γM4, validating previous results found with small lipophilic probes.

The nicotinic acetylcholine receptor (AChR)[1] from the electric organ of *Torpedo californica* is the best characterized member of a superfamily of ligand-gated ion channels which includes the $GABA_A$, glycine, and 5-HT_3 (serotonin) receptors (for recent reviews, see refs *1*−*4*). The *Torpedo* AChR is an integral membrane glycoprotein composed of four homologous subunits in a stoichiometry of $\alpha_2\beta\gamma\delta$ pseudo-symmetrically arranged about a central axis which creates the pore of the cation conducting channel. Each receptor subunit shares identical topologies (*5*, *1*). The N-terminal half of each subunit is extracellular and contains the binding sites for agonist which are located at the interfaces of the α−γ and α−δ subunits. The C-terminal half of each subunit consists of three hydrophobic membrane-spanning segments (M1−M3), a large cytoplasmic domain, a fourth transmembrane segment (M4), and a short C-terminal extracellular tail.

In the absence of a truly high-resolution three-dimensional structure of the AChR (6), investigators have had to rely on a host of different biochemical as well as biophysical approaches to obtain structural information about the receptor. Photoaffinity labeling studies with both AChR agonists and competitive antagonists have been instrumental in identifying amino acid residues involved in forming the agonist-binding site (reviewed in refs *7* and *8*). Affinity-labeling studies with noncompetitive antagonists (NCAs) such as chlorpromazine (CPZ), triphenylmethyl-phosphonium (TPMP), and meproadifen were of central importance in determining that the transmembrane α-helical M2 segment of each receptor subunit forms the lining of the pore of the ion channel (*9*−*13*).

One such noncompetitive antagonist of the AChR which has provided an excellent tool for identifying a number of its important structural features is the hydrophobic, photoreactive compound 3-trifluoromethyl-3-(*m*-[^{125}I]iodophenyl) diazirine ([^{125}I]TID) (14). There are two components to the photoincorporation of TID into the AChR. First, as a potent NCA, TID binds with micromolar affinity to both the resting and desensitized states of the receptor (15). This specific component of [^{125}I]TID incorporation is localized to the channel-lining M2 segments of each receptor subunit and is displaceable by TID itself as well as by other noncompetitive antagonists (*15*−*17*). Second, consistent with the hydro-

[†] This research was supported in part by National Institute of Health NINDS Grant R29 NS35786.

* To whom correspondence should be addressed. Tel: (806) 743-2425. Fax: (806) 743-2744. E-mail: phrmpb@ttuhsc.edu.

[1] Abbreviations: AChR, nicotinic acetylcholine receptor; TTD-BE, 4′-(3-trifluoromethyl-3*H*-diazirin-3-yl)-2′-tributylstannylbenzyl benzoate; TTDPC/16, 1-*O*-hexadecanoyl-2-*O*-[9-[[[2-tributylstannyl)-4-(trifluoromethyl-3*H*-diazirin-3-yl)benzyl]oxy]carbonyl]nonanoyl]-*sn*-glycero-3-phosphocholine; TLC, thin-layer chromatography; [^{125}I]TID, 3-trifluoromethyl-3-(*m*-[^{125}I]iodophenyl) diazirine; VDB, vesicle dialysis buffer (10 mM MOPS, 100 mM NaCl, 0.1 mM EDTA, and 0.02% NaN_3, pH 7.5); SDS, sodium dodecyl sulfate; PAGE, polyacrylamide gel electrophoresis; Tricine, *B*-[2-hydroxy-1,1-bis(hydroxymethyl)ethyl]-glycine; HPLC, high-performance liquid chromatography; V8 protease, *Staphylococcus aureus* V8 protease; kDa, kilodalton; PTH, phenylthiohydantoin.

S0006-2960(98)01435-4 CCC: $15.00
Published on Web 09/25/1998

phobic nature of TID, it partitions extremely effectively into the lipid bilayer and labels regions of the receptor that are exposed to lipid (*18*−*20*). While TID binds to both the resting and desensitized channel with micromolar affinity, [^{125}I]TID photoincorporates into the resting channel with 10-fold greater efficiency. In the resting state, [^{125}I]TID reacts with homologous aliphatic residues in each M2 segment which are located 9 and 13 amino acid residues C-terminal to the conserved lysine residue at the amino terminus of the M2 region (e.g., βLeu-257 and βVal-261). In the presence of agonist, the pattern of [^{125}I]TID incorporation expands to include homologous serine residues at positions 2 and 6 (e.g., βSer-250 and βSer-254). These results provide important information about the NCA-binding site, suggesting that the conserved leucine residues at position 9 (e.g., βLeu-257) may form a permeability barrier to the passage of ions in the resting channel and provide the first direct evidence of an agonist-induced rearrangement of the channel-lining M2 helices. Equally important, the identification of nonspecifically labeled residues in segments M4, M3, and M1 of each subunit define the AChR lipid−protein interface, and the periodicity of [^{125}I]TID-labeled residues indicate that these segments are organized as membrane-spanning α-helices.

The work presented here employs two analogues of TID, a benzoic acid ester ([^{125}I]TID-BE), and a phospholipid ([^{125}I]-TIDPC/16) to obtain additional structural information about the AChR and its conformational states (21). [^{125}I]TID-BE is the first in a potential series of structural analogues of TID which we intend to use to examine the molecular determinants of the noncompetitive antagonist binding site in the AChR channel. For the phospholipid photoreactive probe ([^{125}I]TIDPC/16), the objectives were 2-fold: first, to further evaluate the results obtained from earlier studies identifying lipid-exposed residues in the AChR using small lipophilic probes, and second, due to the location of the photoreactive group at the end of one of the acyl chains of [^{125}I]TIDPC/16, additional information regarding the topological disposition of labeled (lipid-exposed) residues might be obtained.

EXPERIMENTAL PROCEDURES

Materials. AChR-rich membranes were isolated from *T. californica* electric organ (8). Reactivials were purchased from Pierce, silica gel 60 thin-layer chromatography (TLC) plates from Merck, and [^{125}I]Na from American Radiolabeled Chemicals. *S. aureus* V8 protease was purchased from ICN Biochemicals and L-1-tosylamido-2-phenylethyl chloromethyl ketone treated trypsin from Worthington Biochemical Corporation. Genapol C-100 (10%) was purchased from Calbiochem. Prestained low molecular weight gel standards were purchased from Life Technologies, Inc.

[^{125}I]TID-BE and [^{125}I]TIDPC/16. [^{125}I]TID-BE and [^{125}I]-TIDPC/16 were prepared by radioiododestanylation of the tin-based precursors 4′-(3-trifluoromethyl-3*H*-diazirin-3-yl)-2′-tributylstannylbenzyl benzoate (TTD-BE) and 1-*O*-hexadecanoyl-2-*O*-[9-[[[2-tributylstannyl)-4-(trifluoromethyl-3*H*-diazirin-3-yl)benzyl]oxy]carbonyl]nonanoyl]-*sn*-glycero-3-phosphocholine (TTDPC/16), respectively (*22*, *21*). The tin-based precursors were a generous gift from Dr. Josef Brunner of the Swiss Federal Institute of Technology (ETH), Zurich, Switzerland. Briefly, 20 nmol of TTD-BE in ethanol/toulene (1:1) was added to a 1 mL reactivial and dried under nitrogen. The dried material was dissolved in 20 μL of acetic acid, and 2 mCi of [^{125}I]Na was then added and the iodination reaction initiated by the further addition of 5 μL of peracetic acid. After 10 min, the reaction was quenched by adding 3 μL of NaI (100 mM) and 200 μL of sodium bisulfite [10% (w/w)]. The radioidonated compound was extracted into 400 μL of ethyl acetate (upper phase), which was removed and dried under nitrogen. The dried material was dissolved in 100 μL of ethanol/toulene (1:1), applied to a silica gel 60 TLC plate (5 × 20 cm), and developed with ether:hexane (1:9). The position of [^{125}I]TID-BE was determined by autoradiography and by comparison with the migration of TID-BE prepared with nonradioactive iodine. [^{125}I]TID-BE (R_f = 0.7) was scraped from the TLC plate, extracted with 1 mL of ethanol, dried under nitrogen, dissolved in 50 μL of ethanol, and stored at −20 °C. [^{125}I]TIDPC/16 was prepared from its tin-precursor in an identical fashion as that of [^{125}I]TID-BE, with the exception that following the iodination reaction [^{125}I]TIDPC/16 was extracted with 400 μL of chloroform/methanol (2:1), the TLC plate was developed with chloroform/methanol/water/acetic acid (65:25:5:5), and [^{125}I]TIDPC/16 was stored in ethanol/toulene (1:1) at −20 °C.

[^{125}I]TID-BE and [^{125}I]TIDPC/16 Photolabeling of AChR-Rich Membranes. For labeling experiments, *Torpedo* AChR-rich membranes [1 mg/mL in vesicle dialysis buffer (VDB), 10 mM MOPS, 100 mM NaCl, 0.1 mM EDTA, and 0.02% NaN_3, pH 7.5] were incubated for 2 h at room temperature with either [^{125}I]TID-BE or [^{125}I]TIDPC/16 at a final concentration of 0.4 and 0.8 μM, respectively, and with or without 250 μM carbamylcholine chloride. For analytical-labeling experiments, approximately 1 mg of AChR membranes was used and 11−14 mg for preparative labelings. Incubations were performed in either glass test tubes or vials and under reduced lighting conditions. The samples were then irradiated with a 365 nm UV lamp (Spectroline EN-280L) for 7 min at a distance of less than 1 cm, and centrifuged at 39000*g* for 1 h. Pellets were solubilized in electrophoresis sample buffer and counted for 1 min using a Packard Cobra II Gamma Counter before being subjected to SDS−PAGE.

SDS−Polyacrylamide Gel Electrophoresis. SDS−PAGE was performed according to the method of Laemmli (23). Analytical (1.0 mm thick) and preparative (1.5 mm) separating gels were composed of 8% polyacrylamide/0.33% bisacrylamide. Following electrophoresis, gels were stained with Coomassie Blue R-250 to visualize AChR subunit bands. After soaking the gels in distilled water overnight, the α, β, γ, and δ bands for each condition were excised and transferred to either a 1.0 or 1.5 mm (preparative) thick 15% acrylamide mapping gel (*24*, *19*). Each gel slice was overlaid with 4 μg of *S. aureus* V8 protease in overlay buffer (18) or 200 μg of V8 protease for preparative scale mapping gels of the α-subunit (∼14 cm strip). Electrophoresis proceeded at 50 V constant voltage until the tracking dye reached the stacking/separating gel interface (∼3 h) and then at 5 mA constant current overnight. After Coomassie Blue R-250 staining, analytical gels were dried and exposed to Kodak X-OMAT LS film with an intensifying screen at −80 °C. Preparative gels were soaked in distilled water overnight and the 20 kDa (αV8−20, Ser-173−Glu-338) and 10 kDa

(αV8−10, Asn-339−Gly-437) polypeptide bands were excised and, as with the β, γ, and δ subunits from the 8% gels, eluted into 15 mL of elution buffer (0.1 M NH_4HCO_3, 0.1% (w/v) SDS, and 1% β-mercaptoethanol, pH 7.8) for 4 days at room temperature with gentle mixing. The gel suspensions were then filtered through Whatman no. 1 paper and concentrated using a Centriprep-10 (Amicon). Excess SDS was removed by acetone precipitation (∼85% acetone at −20 °C for 12 h).

Isolation of [^{125}I]TID-BE and [^{125}I]TIDPC/16 Labeled Fragments. For digestion with trypsin, acetone-precipitated V8 protease fragments or intact AChR subunits were resuspended in approximately 300 μL of 0.1 M NH_4HCO_3, 0.02% (w/v) SDS, 0.5% Genapol C-100, pH 7.8 (1−2 mg/mL protein). Trypsin was added at a 20% (w/w) enzyme-to-substrate ratio for subunit samples, and 100% (w/w) enzyme-to-substrate ratio for αV8−20 and αV8−10 samples, and the digestion allowed to proceed 4−5 days at room temperature. A small aliquot of each sample was electrophoresed on an analytical (1.0 mm thick) 16.5%T/6%C Tricine SDS−PAGE gel with at least one reference lane containing prestained low molecular weight protein standards (Life Technologies, Inc). The gels were stained, destained, and dried for autoradiography. The bulk of the αV8−20 and αV8−10 tryptic digests were resolved directly by reversed-phase HPLC, while the remainder of the β, γ, and δ tryptic digests were solubilized in electrophoresis sample buffer and submitted to preparative (1.5 mm thick) scale 16.5%T/6%C Tricine gel analysis (*16*, *25*). Prepartive Tricine gels were stained, destained, and soaked in water overnight. Using the autoradiograph from the analytical Tricine gel in conjunction with the prestained protein standards, selected bands (*16*, *25*) were excised and eluted into 4 mL of elution buffer for 4 days at room temperature. Further separation and purification of these samples was accomplished by reversed-phase HPLC using a Brownlee Aquapore C_4 column (100 × 2.1 mm) with solvent A (0.08% TFA in water) and solvent B (0.05% TFA in 60% acetonitrile/40% 2-propanol). A nonlinear elution gradient was employed (25%−100% solvent B in 80 min) and the elution of peptides was monitored by the absorbance at 210 nm. Collected fractions were counted for radioactivity and the peak protein/radioactivity-containing fractions were pooled, dried by vacuum centrifugation, and resuspended in 20 μL of 0.1 M NH_4HCO_3 and 0.1% (w/v) SDS, pH 7.8, for protein microsequence analysis.

Sequence Analysis. Amino-terminal sequence analysis was performed on an Applied Biosystems model 477A protein sequencer using gas-phase cycles (in the lab of Dr. Jonathan B. Cohen, Department of Neurobiology, Harvard Medical School). Peptide aliquots (20 μL) were immobilized on chemically modified glass fiber disks (Beckman Instruments), which were used to improve the sequencing yields of hydrophobic peptides. Approximately 30% of the release PTH-amino acids were separated by an on-line model 120A PTH-amino acid analyzer, and approximately 60% was collected for determination of released ^{125}I by γ-counting of each sample for 20 min. Initial yield (I_o) and repetitive yield (R) were calculated by nonlinear least-squares regression of the observed release (M) for each cycle (n): $M = I_oR^n$ (PTH-derivatives of Ser, Thr, Cys, and His were omitted from the fit).

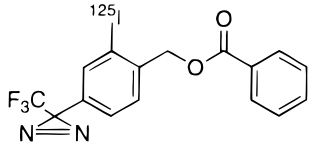

FIGURE 1: Chemical structure of [^{125}I]TID-BE.

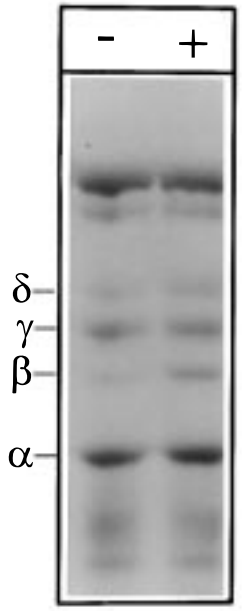

FIGURE 2: Photoincorporation of [^{125}I]TID-BE into AChR-rich membranes in the absence and presence of carbamylcholine. AChR-rich membranes were equilibrated (2 h incubation) with [^{125}I]TID-BE (0.4 μM) in the absence (−lane) and in the presence (+lane) of 250 μM carbamylcholine and irradiated at 365 nm (Spectroline EN-280L) for 7 min (at a distance of <1 cm). Polypeptides were resolved by SDS−PAGE (1.0 mm thick, 8% polyacrylamide gel), visualized by Coomassie Blue R-250 staining and subjected to autoradiography (2−3 day exposure with intensifying screen). Labeled lipid and free photolysis products were electrophoresed from the gel with the tracking dye. The migration of individual AChR subunits are indicated on the left.

RESULTS

[^{125}I]TID-BE Labeling of the AChR. Initial photolabeling experiments were designed to characterize the general pattern of [^{125}I]TID-BE (Figure 1) photoincorporation into the AChR as well as to assess the sensitivity of the labeling to the presence of the AChR agonist carbamylcholine. AChR-rich membranes were equilibrated with [^{125}I]TID-BE (0.4 μM) in the absence and in the presence of 250 μM carbamylcholine, exposed to UV light (365 nm) and the membrane suspensions pelleted. Following centrifugation, greater than 94% of the ^{125}I counts per minute remained with AChR-rich membranes. The membrane pellets were next solubilized in electrophoresis sample buffer and the pattern of incorporation into AChR subunits monitored by SDS−PAGE followed by autoradiography. As is evident in the autoradiograph of an 8% polyacrylamide slab gel (Figure 2), there is appreciable incorporation of [^{125}I]TID-BE into each of the receptor subunits. Upon the basis of γ-counting of excised gel bands, there was approximately equal incorporation of [^{125}I]TID-BE into each of the AChR subunits. The relative ratios are 1:1.1:1.46:1.07 in the absence of agonist and 1:0.98:1.58:1.03 in the presence of 250 μM carbamylcholine (α, β, γ, δ, $n = 4$). Despite the fact that [^{125}I]TID-BE incorporated into each of the AChR subunits in approxi-

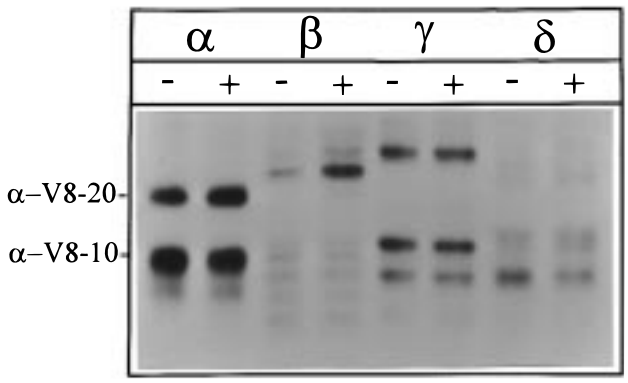

FIGURE 3: Proteolytic mapping of the sites of [^{125}I]TID-BE incorporation into AChR subunits using *S. aureus* V8 protease. AChR-rich membranes were labeled with [^{125}I]TID-BE in the absence (−lanes) or presence (+lanes) of 250 μM carbamylcholine and subjected to SDS−PAGE on a 1.0 mm thick 8% slab gel. AChR subunit bands were excised following identification by staining, transferred to the wells of a 15% mapping gel and overlaid with 6 μg of *S. aureus* V8 protease (see Experimental Procedures). AChR subunits were proteolytically digested as they migrated through the 4.5% acrylamide stacking gel (50 V constant voltage, transit time ~3 h) and the resulting fragments were then resolved on the lower 15% acrylamide separating gel. Following electrophoresis, the mapping gel was stained with Coomassie Blue R-250 and subjected to autoradiography (2 week exposure with intensifying screen). The principal [^{125}I]TID-BE-labeled proteolytic fragments, following the nomenclature of Blanton and Cohen (*20*), are αV8−20 (Ser-173−Glu-338); αV8−10 (Asn-339−Gly-437); βV8−22 (Ile-173/Asn-183− Glu-383); γV8−24 (Ala-167/Trp-170−Glu-372); γV8−14 (Leu-373/Ile-413− Pro-489); γV8−12 (Ala-1 of the β-subunit of the *Torpedo* Na/K ATPase); δV8−12 (Ile-192−Glu-280); δV8−11 (Lys-436−Ala-501).

mately equal abundance, the pattern of incorporation was sensitive to the presence of agonist. In the presence of carbamylcholine (Figure 2, +lane), there is a small but reproducible increase (30%, $n = 6$) in the extent of incorporation into the β-subunit.

[^{125}I]TID-BE incorporation within each of the AChR subunits was examined by limited digestion with *S. aureus* V8 protease in a 15% acrylamide mapping gel (*24*, *26*). Limited V8 digestion reproducibly generates a set of non-overlapping fragments for each receptor subunit (20). Inspection of the autoradiograph of the V8 protease digests (Figure 3) reveals significant [^{125}I]TID-BE incorporation into the following fragments, using the nomenclature of Blanton and Cohen (20): αV8−20 (Ser-173−Glu-338); αV8−10 (Asn-339−Gly-437); βV8−22 (Ile-173/Asn-183−Glu-383); γV8−24 (Ala-167/Trp-170−Glu-372); γV8−14 (Leu-373/Ile-413−Pro-489); γV8−12 (Ala-1 of the β-subunit of the *Torpedo* Na/K ATPase); δV8−12 (Ile-192−Glu-280); δV8−11 (Lys-436−Ala-501). Fragments αV8−20, βV8−22, and γV8−24 are homologous in that they contain the same stretch of amino acid residues in the aligned sequences of each subunit. This stretch contains the transmembrane segments M1, M2, and M3. Similarly, αV8−10, γV8−14, and δV8−11 are also homologous and contain the transmembrane segment M4. The enhanced labeling of the β-subunit when the AChR is labeled in the presence of carbamylcholine maps to the V8 protease fragment βV8−22 (Figure 3, β-subunit lanes). Direct counting of the excised gel bands indicates that in the presence of carbamylcholine there is an approximately 2-fold increase in the extent of [^{125}I]TID-BE incorporation into βV8−22. In contrast, no

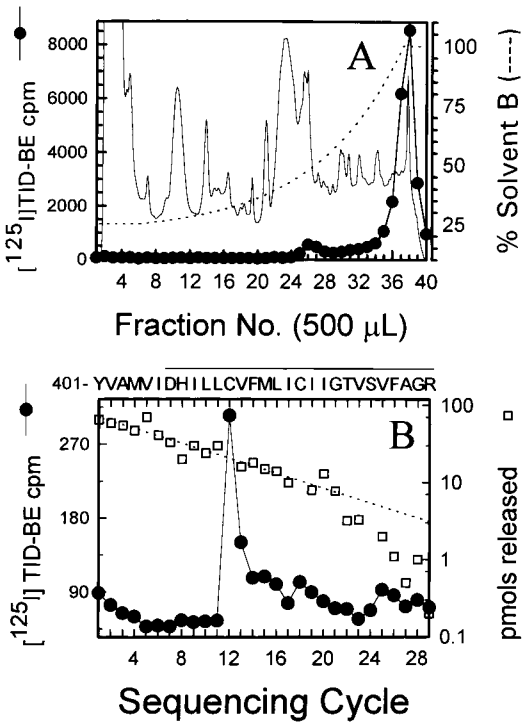

FIGURE 4: Reversed-phase HPLC purification and sequential Edman degradation of a [^{125}I]TID-BE labeled fragment containing αM4. The [^{125}I]TID-BE-labeled 10 kDa V8 protease fragment of the AChR α-subunit (αV8−10, isolated from AChR labeled in the presence of carbamylcholine) was further digested in solution with trypsin and the labeled material purified by reversed-phase HPLC (panel A) on a Brownlee Aquapore C_4 column (100 × 2.1 mm) as described in the Experimental Procedures. The elution of peptides was monitored by absorbance at 210 nm (solid line) and elution of ^{125}I by γ-counting of each 500 μL fraction (●). HPLC fractions 36−39 were pooled and subjected to automated sequential Edman degradation (panel B). Sixty percent of each cycle of Edman degradation was analyzed for released ^{125}I (●) and 30% for released PTH-amino acids (□) with the dashed line corresponding to the exponential decay fit of the amount of detected PTH-amino acids. A primary peptide was detected beginning at Tyr-401 of the α-subunit (initial yield, 78 pmol; repetitive yield, 89.5%; 14 200 cpm loaded on sequencing filter; 6150 cpm remaining after 33 cycles). The amino acid sequence of the peptide is shown above panel B with the solid line indicating the limits of the M4 region.

significant difference (>10%) was detected in the extent of incorporation into any of the other V8 fragments for either the β-subunit or α−α- or δ-subunits. The relative incorporation of [^{125}I]TID-BE into αV8−20/αV8−10 and γV8−24/γV8−14 was very similar for each labeling condition, 46%/54% and 49%/51%, respectively.

Identification of Sites of [^{125}I]TID-BE Incorporation in the M4 Segments of the α- *and* γ*-Subunits.* The M4 segment of the α-subunit was isolated from a tryptic digest of the 10 kDa V8 protease fragment of the α-subunit (αV8−10, Asn-339−Gly-437). The tryptic digest of αV8−10 was separated by reversed-phase HPLC (Figure 4A). In the HPLC chromatogram, there is a single peak of ^{125}I counts per minute (fraction 38) and a corresponding peak in absorbance (93 min). When HPLC fractions 36−39 were pooled and subjected to N-terminal amino acid sequence analysis, the major sequence detected began at αTyr-401 (initial yield, 78 pmol; repetitive yield, 89.5%). In addition to the αTyr-401 sequence, an overlapping fragment beginning at αSer-388 was also detected (initial yield, 54 pmol; repetitive yield, 87.5%). In the ^{125}I release profile shown in Figure 4B, the

largest release occurs in cycle 12, with additional release in cycles 18, 25, and perhaps cycle 15. Comparison of the pattern of release with the corresponding identified amino acids indicates that the labeled residues include αCys-412 (12.2 cpm/pmol), αMet-415, αCys-418, and αVal-425. However, some or all of the release in cycle 25 (αVal-425) may result from release from αCys-412 (11.26 cpm/pmol) in the αSer-388 peptide.

The M4 segment of the γ-subunit was isolated from a tryptic digest of the intact subunit. When the tryptic digest was resolved on a 1.5 mm thick 16.5%T/6%C Tricine SDS−PAGE gel, Coomassie Blue R-250 stained bands migrating with apparent molecular masses of 7 kDa (γT-7K) and 5 kDa (γT-5K), which have previously been shown to contain γM4 (20), were excised. These two fragments are also the most prominently labeled bands present in the autoradiograph of analytical (1.0 mm thick) Tricine SDS−PAGE gel of the [^{125}I]TID-BE labeled γ-subunit tryptic digest. Material eluted from the γT-7K and γT-5K-bands were further purified by reversed-phase HPLC. For γT-7K and γT-5K there were peaks of ^{125}I counts per minute (fractions 37 and 35) and absorbance (90 and 87.5 min), respectively. Fractions 36−38 were pooled for γT-7K and subjected to N-terminal sequence analysis. A single peptide was detected beginning at γGlu-429 and extending through γM4 (initial yield, 53.4 pmol; repetitive yield, 88.2%). Release of ^{125}I in cycle 23 indicated that [^{125}I]TID-BE was incorporated into γCys-451 (10.4 cpm/pmol) within γM4 (7709 cpm loaded; 6509 cpm remaining after 32 cycles). Sequence analysis of the pool of HPLC fractions (fractions 35−38) for γT-5K revealed the presence of a primary sequence beginning at γVal-446, 17 residues C-terminal to the start of γT-7K, and extending through γM4 (initial yield, 26 pmol; repetitive yield, 73%). Release of ^{125}I in cycles 6 and 15 confirmed incorporation of [^{125}I]TID-BE into γCys-451 (10 cpm/pmol) and indicated that there was also incorporation into γSer-460.

Identification of Sites of [^{125}I]TID-BE Incorporation in the M1 Segment of the α-and β-Subunit. The M1 segment of the α-subunit was isolated from a tryptic digest of the 20 kDa V8 protease subunit fragment (αV8−20, Ser-173-Glu-338). The tryptic digest was separated by reversed-phase HPLC (Figure 5A). HPLC fractions 35−37, which contain both a peak of ^{125}I counts per minute (fraction 36) and absorbance (89 min), were pooled based on previous work establishing the point of elution of an ∼3.4 kDa tryptic fragment containing αM1 (27). Sequence analysis of the pooled fractions revealed the presence of a single peptide beginning at αIle-210 (Figure 5B), extending through the transmembrane segment M1 and, in all likelihood, terminating at αLys-242, which is at the amino-terminal end of the M2 segment (initial yield, 47 pmol; repetitive yield, 92.9%). The ^{125}I released in cycles 18 and 19 is consistent with [^{125}I]-TID-BE incorporation into αPhe-227 and αLeu-228 within the M1 segment of the α-subunit (1400 cpm loaded onto filter; 689 cpm remaining after 30 cycles).

The M1 segment of the β-subunit was isolated from a tryptic digest of the intact subunit. When the tryptic digest was resolved on a 1.5 mm thick 16.5%T/6%C Tricine SDS−PAGE gel, a Coomassie Blue R-250 stained band migrating with an apparent molecular weight of 10 kDa (βT-10K), and which was previously shown to begin at βLys-216 and contain the M1-M2-M3 segments of the β-subunit (*16*, *27*),

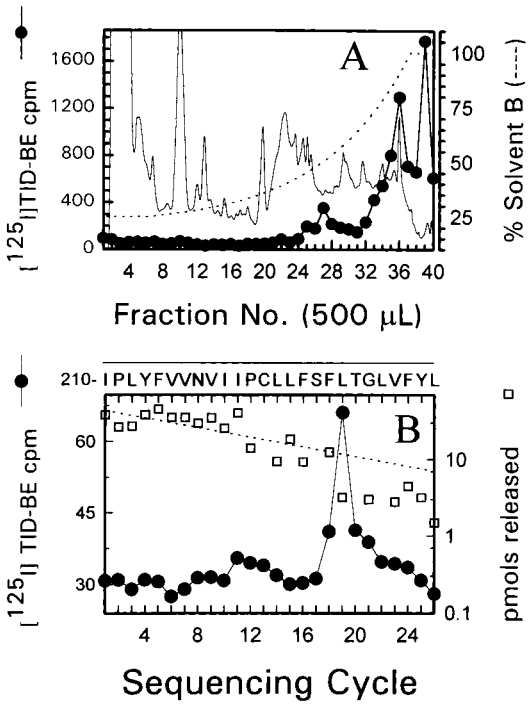

FIGURE 5: Reversed-phase HPLC purification and sequential Edman degradation of a [^{125}I]TID-BE labeled fragment containing αM1. The [^{125}I]TID-BE-labeled 20 kDa V8 protease fragment of the AChR α-subunit (αV8−20; labeled in the presence of carbamylcholine) was further digested in solution with trypsin and the labeled material purified by reversed-phase HPLC (panel A) as described in the Experimental Procedures and in the legend for Figure 4. Elution of ^{125}I was determined by γ-counting of each 500 μL fraction (●) and the elution of peptides by absorbance at 210 nm (solid line). HPLC fractions 35−37, corresponding to a peak of ^{125}I counts per minute and absorbance (∼89 min) were pooled and subjected to automated sequential Edman degradation (panel B). Thirty percent of each cycle of Edman degradation was analyzed for released PTH-amino acids (□) and 60% for released ^{125}I (●). A single peptide was detected beginning at Ile-210 of the α-subunit (initial yield, 47 pmol; repetitive yield, 92.9%; 1400 cpm loaded on sequencing filter; 689 cpm remaining after 30 cycles). In panel B, the dashed line corresponds to the exponential decay fit of the amount of detected PTH-amino acids and the solid line above the amino acid sequence indicates the limits of the M1 region.

was excised. Material eluted from the βT−10K band was further purified by reversed-phase HPLC and the pooled fractions (38−40) were sequenced. Sequence analysis revealed the presence of a single peptide beginning at βLys-216 (initial yield, 20 pmol; repetitive yield, 92%) with ^{125}I release in cycles 19 and 20 (2200 cpm loaded, 1350 cpm remaining after 26 cycles). Comparison of the pattern of ^{125}I release with the corresponding identified amino acids indicate that βLeu-234 and βAla-235 are the primary sites of [^{125}I]TID-BE labeling in βM1.

Identification of the Sites of [^{125}I]TID-BE Incorporation in βM2. The β-subunits isolated from AChRs labeled with [^{125}I]TID-BE in the absence and in the presence of 250 μM carbamylcholine were digested with 20% (w/w) trypsin for 4 days. An aliquot of each digest was resolved on a 1.0 mm thick 16.5%T/6%C Tricine SDS−PAGE gel. The corresponding autoradiograph revealed the presence of two bands migrating with apparent molecular weights of 10 kDa (βT−10K) and 7 kDa (βT−7.7K) in which there was enhanced labeling in the presence of carbamylcholine. These fragments have been identified in previous studies (*16*, *25*).

The amino-terminus of βT−10K is βLys-216, with the peptide extending through transmembrane segments M1, M2 and M3, and terminating at or near βArg-307 (M1−M2−M3). The C-terminus of βT−7.7K is also likely to be at or near βArg-307, while the amino-terminus, βMet-249, is at the N-terminal end of the M2 segment (M2−M3). In the autoradiograph of the β-subunit digest, the lack of carbamylcholine-enhanced labeling of an approximately 5 kDa fragment (βT−5K), known to contain only the transmembrane segment M1 (unpublished results), indicates that the agonist-sensitive [^{125}I]TID-BE labeling is contained within either the M2 or M3 transmembrane segment.

When the bulk of the tryptic digests of the β-subunit was resolved on 1.5 mm thick Tricine SDS−PAGE gels, the βT−7.7K fragment from each labeling condition were isolated and the eluted material further purified by reversed-phase HPLC. For each labeling condition, the majority of ^{125}I counts eluted in a peak contained in fraction 37 with a corresponding peak of absorbance eluting at 93 min. HPLC fractions 36−39 were pooled and subjected to N-terminal sequence analysis (Figure 6). In each labeling condition, sequence analysis revealed the presence of a major sequence beginning at βMet-249 of the β-subunit, present at nearly identical mass levels and that sequenced with similar efficiency (initial yields of 21, 22 pmol; repetitive yields of 93.3 and 93.6%). In each condition, a minor sequence beginning at βSer-199 was also present at about one-quarter the amount of the βMet-249 peptide. For the sample labeled in the absence of agonist (Figure 6A), there was no significant release of ^{125}I counts per minute (above background) in any of the 20 sequencing cycles (2420 cpm loaded; 2150 cpm remaining after 20 cycles). While there were no apparent sites of [^{125}I]TID-BE incorporation into βM2 (labeled in the absence of carbamylcholine), the ^{125}I counts per minute associated with the βT−7.7K fragment suggests that there are sites of labeling further downstream (C-terminal) of the M2 segment, in all likelihood within the M3 segment. For the βT−7.7K sample labeled in the presence of agonist (Figure 6B), there are sites of ^{125}I release in cycles 9, 13, and 16 (5519 cpm loaded on sequencing filter; 3409 cpm remaining after 34 cycles). The pattern of ^{125}I release corresponds to [^{125}I]TID-BE incorporation into βLeu-257 (0.66 cpm/pmol), βLeu-264 (0.6 cpm/pmol), and the primary site of labeling βVal-261 (1.52 cpm/pmol). In addition, while the levels of ^{125}I counts per minute in cycles 10−12 are elevated above that of the background observed in cycles 1−8, it is unclear whether this is the result of increased wash-off of the labeled peptide, preview of the release in cycle 13, or incorporation into one or more of the corresponding βM2 residues (βAla-258, βVal-259, βThr-260).

[^{125}I]TIDPC/16 Labeling of the AChR. Initial photolabeling experiments were designed to assess the ability to introduce the phospholipid probe (ethanolic stock solution) by simple incubation with AChR-rich membranes as well as to characterize the general pattern and agonist-sensitivity of [^{125}I]TIDPC/16 (Figure 7) photoincorporation into the AChR. AChR-rich membranes were equilibrated for increasing periods of time with [^{125}I]TIDPC/16 (0.8 μM) in the absence and in the presence of 250 μM carbamylcholine, exposed to UV light (365 nm) and the membrane suspensions pelleted. With a 2 h incubation, greater than 86% of the

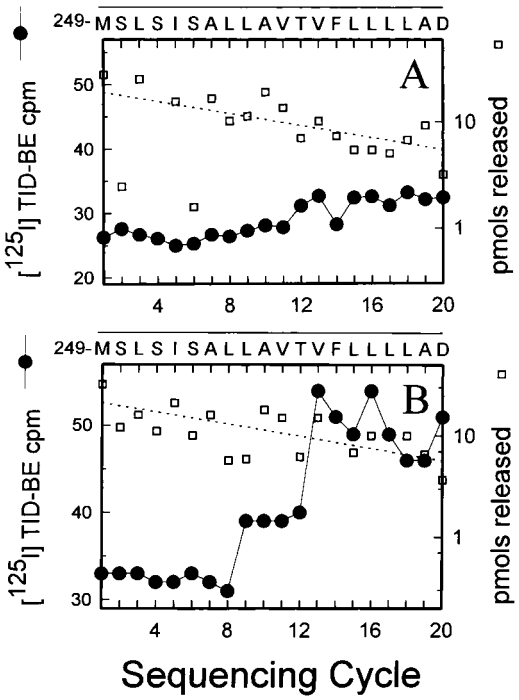

FIGURE 6: Radioactivity and mass release upon amino-terminal sequence analysis of a [^{125}I]TID-BE labeled fragment containing βM2. The AChR β-subunit isolated from receptors labeled in the presence and absence of carbamylcholine was digested in solution with trypsin, the digests separated on 1.5 mm thick 16.5%T/6%C Tricine SDS−PAGE gels and an approximately 7.7 kDa fragment (βT−7.7K) isolated (see Experimental Procedures). The βT−7.7K fragment was further purified by reversed-phase HPLC with fractions 36−39 pooled and subjected to automated Edman degradation.. Sixty percent of each cycle of Edman degradation was analyzed for released ^{125}I (●) and 30% for released PTH-amino acids (□) with the dashed line corresponding to the exponential decay fit of the amount of detected PTH-amino acids. The amino acid sequence of the sequenced peptide containing the M2 region is shown above each panel. (Panel A) ^{125}I release from βT−7.7K labeled in the absence of carbamylcholine (initial yield, 21 pmol; repetitive yield, 93.6%; 2420 cpm loaded on sequencing filter; 2150 cpm remaining after 20 cycles). (Panel B) ^{125}I release from βT−7.7K labeled in the presence of carbamylcholine (initial yield, 22 pmol; repetitive yield, 93.3%; 5519 cpm loaded on sequencing filter; 3409 cpm remaining after 20 cycles).

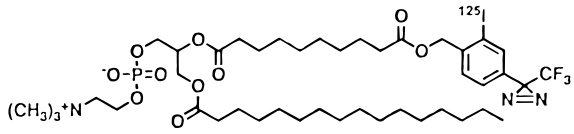

FIGURE 7: Chemical structure of [^{125}I]TIDPC/16.

^{125}I counts per minute remained with AChR-rich membranes and longer incubation times of up to 20 h resulted in only a minor increase in the extent of [^{125}I]TIDPC/16 membrane partitioning.[2] Following centrifugation and γ-counting,

[2] The pattern of [^{125}I]TIDPC/16, [^{125}I]TID, and [^{125}I]TID-BE incorporation into AChR subunits and subunit proteolytic fragments was also determined under conditions in which the photoreactive probe was incubated with detergent (cholate) solubilized receptors and with or without carbamylcholine. The pattern and extent of labeling for each photoreactive compound was found to be identical to that observed when the probe was added to AChR-rich membranes. One implication of these results is that it indicates that cholate solubilized AChRs are still capable of undergoing agonist-induced conformational transitions and that in the absence of agonist the receptor remains in the resting state.

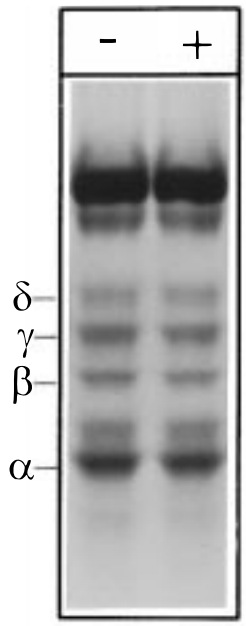

FIGURE 8: Photoincorporation of [^{125}I]TIDPC/16 into AChR-rich membranes in the absence and presence of carbamylcholine. AChR-rich membranes were equilibrated (2 h incubation) with [^{125}I]-TIDPC/16 (0.8 μM) in the absence (−lane) and in the presence (+lane) of 250 μM carbamylcholine and irradiated at 365 nm for 7 min. Polypeptides were resolved by SDS−PAGE (1.0 mm thick, 8% polyacrylamide gel), visualized by Coomassie Blue R-250 staining and subjected to autoradiography (24 h exposure with intensifying screen). Labeled lipid and free photolysis products were electrophoresed from the gel with the tracking dye. The migration of individual AChR subunits are indicated on the left. Significant [^{125}I]TIDPC/16 incorporation is also evident in the α-subunit of the Na/K ATPase (∼95 kDa) and in the CLC-0 chloride channel (∼90 kDa).

membrane pellets were solubilized in electrophoresis sample buffer and the pattern of incorporation into AChR subunits monitored by SDS−PAGE followed by autoradiography. The autoradiograph of an 8% polyacrylamide slab gel (Figure 8) reveals that there is substantial incorporation of [^{125}I]TIDPC/16 into each of the AChR subunits. In addition to the AChR subunits, there is also labeling of the receptor-associated peripheral protein, Rapsyn, of M_r 43000 (28) which migrates with slightly slower electrophoretic mobility than the α-subunit. There is also substantial [^{125}I]TIDPC/16 incorporation into the α-subunit of the Na/K ATPase (∼95 kDa) and to a lesser extent into the CLC-0 chloride channel protein (∼89 kDa). Neither the pattern of incorporation into individual AChR subunits nor the overall labeling pattern was effected by inclusion of 250 μM carbamylcholine (Figure 8, +lane). Upon the basis of γ-counting of excised gel bands, the relative incorporation of [^{125}I]TIDPC/16 into the AChR subunits is 0.57:1.05:1:1.07 in the absence of agonist and 0.58:1.05:1:0.92 in the presence of 250 μM carbamylcholine (α, β, γ, δ, $n = 4$).

[^{125}I]TIDPC/16 incorporation within each of the AChR subunits was next mapped by limited enzymatic digestion with *S. aureus* V8 protease (*24*, *26*). As described previously, limited V8 digestion reproducibly generates a set of nonoverlapping fragments for each receptor subunit (20). Inspection of the autoradiograph of the 15% acrylamide mapping gel containing the V8 protease digests of each receptor subunit (Figure 9) reveals significant [^{125}I]TIDPC/16 incorporation into the following fragments: αV8−20; αV8−10; βV8−22; γV8−24; γV8−14; γV8−12; δV8−12; and δV8−11 (see the legend for Figure 3 for more detail). Direct counting of the excised gel bands did not reveal any significant difference (>5%) in the extent of [^{125}I]-TIDPC/16 incorporation into any of the AChR subunit V8 protease fragments. Of the four fragments generated by V8 digestion of the AChR α-subunit [αV8−20, Ser-173−Glu-338; αV8−18, Thr-52−Glu-172; αV8−10, Asn-339−Gly-437; and αV8−4, Ser-1−Glu-51 (26)] greater than 92% of the ^{125}I counts per minute was contained within αV8−20 and αV8−10, the relative incorporation being 42 and 58%, respectively. The homologous set of fragments generated by V8 protease digestion of the γ-subunit, γV8−24/γV8−14, incorporated [^{125}I]TIDPC/16 in relative amounts that were nearly identical (41 and 59%, respectively) to that of αV8−20 and αV8−10.

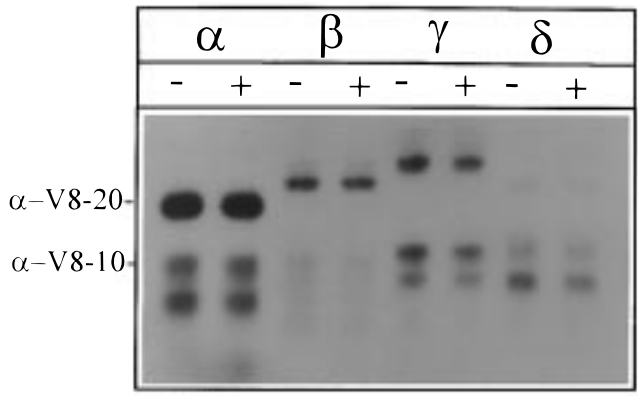

FIGURE 9: Proteolytic mapping of the sites of [^{125}I]TIDPC/16 incorporation into AChR subunits using *S. aureus* V8 protease. AChR-rich membranes were labeled with [^{125}I]TIDPC/16 in the absence (−lanes) or presence (+lanes) of 250 μM carbamylcholine and subjected to SDS−PAGE on a 1.0 mm thick 8% polyacrylamide slab gel. [^{125}I]TIDPC/16-labeled AChR subunit bands were excised for digestion with 6 μg of *S. aureus* V8 protease in a proteolytic mapping gel as described in the Experimental Procedures and in the legend to Figure 3. The mapping gel was stained with Coomassie Blue R-250 and subjected to autoradiography (1 week exposure with intensifying screen). The principal [^{125}I]TIDPC/16-labeled fragments are αV8−20; αV8−10; βV8−22; γV8−24; γV8−14; γV8−12; δV8−12; and δV8−11 (see legend to Figure 3).

Mapping the Sites of [^{125}I]TIDPC/16 Incorporation to the M4 Segments of the α- and γ-Subunits. The M4 segment of the α- and γ-subunits was isolated from tryptic digests of αV8−10 (Asn-339−Gly-437) and γV8−14 (Leu-373−Pro-489). The tryptic digest of αV8−10 was separated by reversed-phase HPLC and the M4 peptide eluted as a single peak of ^{125}I counts per minute (fraction 38) and a corresponding peak in absorbance (92.5 min). In the HPLC chromatogram of the tryptic digest of γV8−14, the γM4 peptide eluted in a peak of ^{125}I counts per minute (fraction 36/37) and absorbance (90 min). When HPLC fractions 36−39 were pooled for the tryptic digest of αV8−10 and subjected to N-terminal amino acid sequence analysis, the major sequence detected began at αTyr-401 (initial yield, 89 pmol; repetitive yield, 93%). In the ^{125}I release profile, there was sporadic release of counts throughout the 30 sequencing cycles. While the primary site of release was in cycle 12 (0.32 cpm/pmol) corresponding to [^{125}I]TIDPC/16 incorporation into αCys-412 in αM4, the complex labeling pattern did not allow for a definitive identification of any

one site of labeling. This result was not entirely unexpected; there was considerable concern that because of the zwitterionic nature of [^{125}I]TIDPC/16, labeled amino acid residues might not be efficiently extracted by the solvents used in automated Edman degradation (Dr. J. Brunner, personnal communication). Sequence analysis of the pool of HPLC fractions (35−39) for the tryptic digest of γV8−14 resulted in a similar ^{125}I release profile. Despite the presence of a fairly abundant peptide beginning at γVal-446 and which sequenced with high efficiency (initial yield, 45 pmol; repetitive yield, 92%), there was sporadic release of ^{125}I counts per minute with no clear primary site of incorporation.

The M1 segment of the α-subunit was isolated from a tryptic digest of αV8−20 (Ser-173−Glu-338). The digest was resolved by reversed-phase HPLC with a peak of ^{125}I counts per minute in fraction 37 and a corresponding peak in absorbance eluting at 91 min. HPLC fractions 36−38 were pooled and sequenced for five cycles in order to confirm the identity of the labeled peptide (αM1, Ile-210-Lys-242).

DISCUSSION

The purpose of the work presented here was to probe the structure of both the AChR ion channel as well as lipid−protein interface with the hydrophobic photoreactive compounds [^{125}I]TID-BE and [^{125}I]TIDPC/16. For both probes, the majority of photoincorporation into the AChR was insensitive to the presence of agonist, hence, the labeling was the same in either the resting or the desensitized conformational state of the receptor. The agonist-insensitive labeling for both [^{125}I]TID-BE and [^{125}I]TIDPC/16 mapped to regions and individual amino acid residues which previous studies have shown are exposed to the lipid bilayer (reviewed in ref *25*). In addition, for [^{125}I]TID-BE, there was enhanced labeling (∼30%) of the β-subunit when the AChR was labeled in the presence of agonist and this agonist-induced labeling was restricted to residues in the channel lining βM2 segment. Thus, there exist two components to the labeling of the AChR by [^{125}I]TID-BE: an agonist-insensitive component consistent with incorporation into residues situated at the receptor lipid−protein interface and a specific, agonist-induced component reflecting labeling of the desensitized conformation of the AChR ion channel.

Agonist-Induced [^{125}I]TID-BE Photoincorporation into βM2. In the absence of agonist, 3-trifluoromethyl-3-(*m*-[^{125}I]-iodophenyl)diazirine ([^{125}I]TID), the parent compound for [^{125}I]TID-BE, photoincorporates extremely efficiently into homologous aliphatic residues (e.g., βLeu-257, β-Val-261) in the channel-lining M2 segments of each AChR subunit (16). At the subunit level, greater than 70% of the total [^{125}I]-TID labeling reflects incorporation into the M2 segments. In contrast, there was no detectable [^{125}I]TID-BE photoincorporation into any residue within the M2 segment of the β-subunit. Furthermore, addition of nonradioactive TID-BE had very little effect on the extent of photoincorporation of [^{125}I]TID into the resting AChR (IC_{50} > 120 μM; data not shown). While TID binds to the AChR channel with micromolar affinity (15), these results indicate that TID-BE binds to the channel very weakly if at all. The inability of TID-BE to interact with the resting channel is not apparently a simple reflection of a difference in the size of the two compounds. The hydrophobic photoreactive compound, [^{3}H]-diazofluorene (DAF), is similar in size to [^{125}I]TID-BE, yet binds with micromolar affinity to the resting AChR channel, photoincorporating into βVal-261 and δVal-269 within the M2 segment of the β- and δ-subunits (25). Clearly, the physiochemical differences between TID and TID-BE are critically important for binding to the pore of the resting ion channel. These differences provide important clues about the molecular environment of the ligand-binding site and insight regarding the binding site determinants. Among the possible explanations for the differences in binding affinity is that either the polarity of the ester linkage and/or the increased torsional flexibility of the molecule introduced by the ester linkage adversely affects the interaction of TID-BE with the resting channel pore. Along these lines, we are currently examining the pattern of photoincorporation into the AChR of both an alcohol ([^{125}I]TIDBA) and an acetate ([^{125}I]TIDBAc) derivative of [^{125}I]TID (21). Preliminary studies indicate that [^{125}I]TID and its alcohol analogue ([^{125}I]TIDBA) interact with the resting AChR channel in a similiar fashion: (1) the pattern and extent of incorporation into AChR subunits is nearly identical for the two probes as is the sensitivity of the labeling to the addition of the agonist carbamylcholine; (2) nonradioactive TIDBA inhibits [^{125}I]TID photoincorporation into the resting AChR in a dose-dependent fashion (IC_{50} = 4.8 μM) with a reported K_i value for nonradioactive TID inhibition of 4 μM (15); (3) Finally, the AChR NCA 3,4,5-trimethoxybenzoic acid 8-(diethylamino) ocytl ester (TMB-8) inhibits photoincorporation of both [^{125}I]TIDBA and [^{125}I]TID into the AChR γ-subunit by greater than 85% and with nearly identical IC_{50} values, 2.75 and 3.1 μM, respectively. Examination of the interaction of the acetate analogue of TID ([^{125}I]TIDBAc) with the AChR will likely provide critical information regarding the stucture−activity relationship for TID binding to the resting channel.

In the presence of agonist, [^{125}I]TID-BE photoincorporates into the aliphatic residues βLeu-257, βVal-261, and βLeu-264 in the M2 region of the AChR β-subunit. Under nearly identical labeling conditions, [^{125}I]TID incorporates into βSer-250, βSer-254, βLeu-257, and βVal-261 (16).[3] As illustrated in Figure 10, for each photoreactive probe, labeled residues are located over a fairly broad expanse of the M2 segment, between three and four consecutive α-helical turns. It is also evident, that while the binding sites for TID and TID-BE overlap, the binding loci for TID-BE is located closer to the extracellular end of the M2 segment (i.e., channel pore). These results reinforce earlier conclusions that different NCAs bind to unique regions of the channel pore even when the AChR is in the same conformational state (reviewed in ref *7*). For example, in the desensitized channel, NCAs such as TID (16) and chlorpromazine (*9*−*11*) bind close to the intracellular end of the channel (i.e., near βSer-250 and βSer-254), TID-BE and DAF (25) bind closer to the middle or upper half of the channel (i.e., near βLeu-257, βVal-261, and βLeu-264), and finally, the NCA meproadifen (13) binds

[3] An alternative explanation for [^{125}I]TID labeling of βLeu-257 and βVal-261 in the presence of agonist (50 μM carbamylcholine) is the presence of a small fraction (<10%) of AChRs remaining in the resting state. The observed [^{125}I]TID labeling pattern would then reflect a mixture of patterns resulting from AChRs in both the resting and desensitized state. With labeling of βSer-250 and βSer-254 in βM2 resulting from [^{125}I]TID binding to the desensitized channel (*16*).

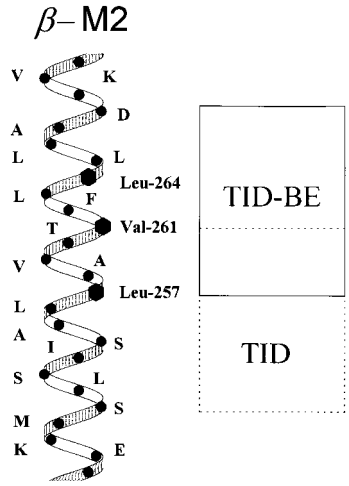

FIGURE 10: Helical representation of the βM2 segment with the binding loci of TID and TID-BE indicated. A helical representation of the M2 segment of the AChR β-subunit is shown. Amino acids which incorporate [^{125}I]TID-BE when the AChR is labeled in the presence of agonist, i.e., the desensitized state, include (βLeu-257, βVal-261, and βLeu-264); those labeled by [^{125}I]TID in the presence of carbamylcholine include [βSer-250, βSer-254, βLeu-257, and βVal-261 (*16*)]. The βM2 helix is oriented with the N-terminus at the bottom reflecting the extracellular location of the carboxy-terminus. The solid and dotted boxes to the right of the M2-helix are meant to illustrate that TID-BE and TID, respectively, have unique though overlapping binding site loci.

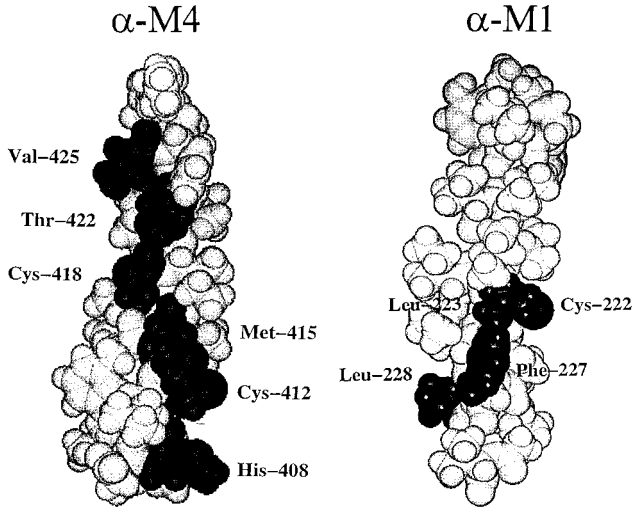

FIGURE 11: CPK model of the αM4 and αM1 helices with [^{125}I]-TID-labeled amino acid residues. CPK helical representations of the αM4 and αM1 regions indicating the residues previously shown to be labeled by [^{125}I]TID [shaded (*20*)]. The model illustrates that the residues labeled by [^{125}I]TID-BE in αM4 (Cys-412, Met-415, and Cys-418) and in αM1 (Phe-227 and Leu-228) represent a subset of the [^{125}I]TID-labeled, lipid-exposed residues in each transmembrane helix. Note: αHis-408 is not labeled by [^{125}I]TID but has been identified as a lipid-exposed residue by reaction with other lipophilic probes (*25*, *29*).

near the extracellular end of the channel (i.e., near βAsp-268). It is also noteworthy that the enhanced labeling of the AChR observed in the presence of agonist is restricted to the M2 segment of the β-subunit. While it is possible that the M2 segments of the α-, γ-, and δ-subunits also incorporate [^{125}I]TID-BE at some low level, residues within βM2 are nonetheless preferentially labeled. This result is surprising given that, for the residues labeled by [^{125}I]TID-BE in βM2 (βLeu-257, βVal-261, and βLeu-264), identical residues are present at the homologous positions in the M2 segment of the α- and δ-subunits. The preferential labeling of βM2 residues is then not likely the result of differences in the reactivity of these residues in the other M2 segments, rather it indicates that within the pore of the ion channel the photoreactive diazirine moiety of [^{125}I]TID-BE is preferentially oriented toward βM2. This result suggests the presence of a certain degree of structural asymmetry within the pore of the desensitized channel. A similar conclusion was reached about the structure of the resting ion channel based on the pattern of M2 labeling by the uncharged photoreactive NCA, [^{3}H]DAF (25).

Characterization of [^{125}I]TID-BE and [^{125}I]TIDPC/16 Labeling at the AChR Lipid−Protein Interface. The majority of labeling of the AChR by either [^{125}I]TID-BE or [^{125}I]-TIDPC/16 is insensitive to the presence of agonist and appears similar to the component of labeling for both [^{125}I]-TID (20) and [^{3}H]DAF (25) that is neither affected by the presence or absence of agonist nor inhibitable by excess nonradioactive ligand, a component which is consistent with labeling of regions/amino acid residues which are in contact with lipid.

Residues incorporating [^{125}I]TID-BE in the M4 segments of the α- and γ-subunit were determined. In αM4, [^{125}I]-TID-BE reacted with Cys-412, Met-415, and Cys-418 (Figure 4B) and in γ-M4, with Cys-451 and Ser-460. As illustrated in Figure 11, the residues labeled by [^{125}I]TID-BE in α-M4 (and in γ-M4) represent a subset of the residues previously identified for [^{125}I]TID incorporation into M4 segments (20). For both αM4 and γM4, [^{125}I]TID-BE-labeled residues are situated within the same lipid-exposed face of each α-helix (Figure 11) identified by the lipophilic probes [^{125}I]TID (20), [^{3}H]diazofluorene (25), and [^{3}H]promegestone (29). As with each of these other probes, positional effects rather than the intrinsic reactivity of the side chains of individual amino acid residues have a dominant effect on the pattern of [^{125}I]TID-BE incorporation. For example, in αM4 [^{125}I]TID-BE reacts with Cys-412 (12.2 cpm/pmol) with 5-fold greater efficiency than with Cys-418 (2.47 cpm/pmol). One interpretation of these results is that TID-BE as well as other lipophilic probes tend to orient in the bilayer and /or preferentially interact with this region in each of the M4 segments.

It was hoped that the phospholipid analogue of TID ([^{125}I]-TIDPC/16) might provide additional topological information regarding the disposition of some of these labeled (lipid-exposed) residues relative to that of the lipid bilayer. Within [^{125}I]TIDPC/16, the photoreactive group is located at the end of one of the fatty acyl chains and in the lipid bilayer would be situated near the center of the bilayer. While it is likely that the fatty acyl-attached photoreactive TID group would have some transverse mobility in the lipid bilayer, the expectation was that the pattern of [^{125}I]TIDPC/16 incorporation into residues in the M4 segment would at least partially reflect the transbilayer disposition of the labeled residues. Unfortunately, while [^{125}I]TIDPC/16 incorporation into the AChR was mapped to the confines of at least the M4 segment of the α- and γ-subunit (as well as αM1), due to technical reasons it was not possible to obtain information about incorporation into individual residues using automated N-terminal sequence analysis. We are currently exploring alternative strategies for determining which residues within these transmembrane segments are labeled by [^{125}I]TIDPC/

16. Nonetheless, that the sites of [^{125}I]TIDPC/16 incorporation map to the same transmembrane segments previously identified using small lipophilic probes such as [^{125}I]TID and [^{3}H]DAF provides further validation of the results obtained with these probes, and, diminishes the possibility that these small lipophilic probes are identifying hydrophobic pockets as opposed to regions which are directly in contact with lipid.

In the M1 segments of the α- and β-subunits, it was determined that [^{125}I]TID-BE reacted with αPhe-227, αLeu-228 (Figure 5B, αM1) and βleu-234, βAla-235 (βM1). As is illustrated in Figure 11, the residues which incorporate [^{125}I]TID-BE in αM1 represent a subset of the residues previously shown to be labeled by [^{125}I]TID (20). As with TID (αM1), the [^{125}I]TID-BE labeled residues are located in the C-terminal portion of the αM1 and βM1 segments (after αPro-221), suggesting that only this part of M1 is exposed to lipid. While it does not provide direct support, this conclusion is also consistent with the results of Akabas and Karlin (30) which indicate that select residues in the amino-terminal third of αM1 and βM1 (31) are exposed to the aqueous lumen of the ion channel pore. It is particularly striking there is no detectable [^{125}I]TID-BE incorporation into αCys-222, as this residue was labeled by [^{125}I]TID and cysteine residues are extremely reactive to diazirines (32). The implication of this result is that the larger TID-BE molecule is restricted in how it can interact with the lipid-exposed portion of the M1 segment. [^{125}I]TID-BE can only associate with the M1 segment with the photoreactive diazirine group oriented away from (αCys-222 and αLeu-223) and toward (αPhe-227 and αLeu-228). Given the limited lipid exposure of the M1 segment and that the extracellular portion of M1 is exposed to the channel lumen as well as presumably making protein:protein contacts, it is tempting to speculate that the labeled portion of the M1 segment may represent a lipid-exposed pocket.

Finally, from the limited number of labeled residues in either αM1 or βM1, no definitive conclusion can be reached regarding the secondary structure of the M1 segment, which may represent either a distorted α-helix (27) or β-sheet (6) and contain stretches of unordered secondary structure (*30*, *33*, *34*).

CONCLUSIONS

Our results demonstrate that there are two components to the labeling of the AChR for both TID and TID-BE: a specific agonist-sensitive component reflecting labeling of the channel-lining M2 segments and a nonspecific agonist-insensitive component consistent with incorporation into residues situated at the lipid−protein interface. Only the latter component is present for the phospholipid analogue of TID ([^{125}I]TIDPC/16). While TID, TID-BE, and TIDPC/16 interact in a similar fashion with the transmembrane segments of the AChR which are in contact with lipid, TID and TID-BE interact very differently with the AChR ion channel. While TID binds with micromolar affinity to the resting channel, photoincorporating with high efficiency into M2 residues, TID-BE does not appear to bind to the resting channel. Both TID and TID-BE bind to the channel in the desensitized state, however, the two compounds have distinct binding loci with TID-BE binding closer to the extracellular end of the channel. These differences provide important clues about the structure and environment of the binding site(s) for noncompetitive antagonists in both the resting and desensitized channel and provide the foundation for future studies aimed at better understanding the molecular determinants of the NCA-binding site.

ACKNOWLEDGMENT

We thank Dr. Josef Brunner (Swiss Federal Institute of Technology Zurich, Zurich, Switzerland) for kindly providing the tin-precursors of [^{125}I]TID-BE and [^{125}I]TIDPC/16 and for his invaluable insight. We also thank Drs. Jonathan B. Cohen and David C. Chiara (Harvard Medical School) for graciously making available the critically important N-terminal radio-sequencing services.

REFERENCES

1. Hucho, F., Tsetlin, V. I., and Machold, J. (1996) *Eur. J. Biochem. 239*, 539−557.
2. Smith, G. B. and Olsen, R. W. (1995) *Trends Pharmacol. Sci. 16*, 162−168.
3. Jackson, M. B. and Yakel, J. L. (1995) *Annu. Rev. Physiol. 57*, 447−68.
4. Kuhse, J., Betz, H., and Kirsch, J. (1995) *Curr. Opin. Neurobiol. 5*, 318−323.
5. Conti-Tronconi, B. M., McLane, K. E., Raftery, M. A., Grando, S. A., and Protti, M. P. (1994) *Crit. Rev. Biochem. Mol. Bio. 29*, 69−123.
6. Unwin, N. (1993) *J. Mol. Biol. 229*, 1101−1124.
7. Galzi, J.-L., and Changeux, J.-P. (1995) *Neuropharmacology 34*, 563−582.
8. Chiara, D. C., and Cohen, J. B. (1997) *J. Biol. Chem. 272*, 32940−32950.
9. Giraudat, J., Dennis, M., Heidmann, T., Chang, J., and Changeux, J. P. (1986) *Proc. Natl. Acad. Sci. U.S.A. 83*, 2719−2723.
10. Giraudat, J., Galzi, J.-L., Revah, F., Changeux, J.-P., Haumont, P.-Y., and Lederer, F. (1989) *FEBS Lett. 253*, 190−198.
11. Revah, F., Galzi, J.-L., Giraudat, J., Haumont, P.-Y., Lederer, F., and Changeux, J.-P. (1990) *Proc. Natl. Acad. Sci. U.S.A. 87*, 4675−4679.
12. Hucho, F. (1986) *Eur. J. Biochem. 158*, 211−226.
13. Pedersen, S. E., Sharp, S. D., Liu, W.-S., and Cohen, J. B. (1992) *J. Biol. Chem. 267*, 10489−10499.
14. Brunner, J., and Semenza, G. (1981) *Biochemistry 20*, 7174−7182.
15. White, B. H., Howard, S., Cohen, S. G., and Cohen, J. B. (1991) *J. Biol. Chem. 266*, 21595−21607.
16. White, B. H., and Cohen, J. B. (1992) *J. Biol. Chem. 267*, 15770−15783.
17. Moore, M. A., and McCarthy, M. P. (1994) *Biochim. Biophys. Acta 1190*, 457−464.
18. White, B. H., and Cohen, J. B. (1988) *Biochemistry 27*, 8741−8751.
19. Blanton, M. P., and Cohen, J. B. (1992) *Biochemistry 31*, 3738−3750.
20. Blanton, M. P., and Cohen, J. B. (1994) *Biochemistry 33*, 2859−2872.
21. Weber, T., and Brunner, J. (1995) *J. Am. Chem. Soc. 117*, 3084−3095.
22. Eichler, J., Brunner, J., and Wickner, W. (1997) *EMBO J. 16*, 2188−2196.
23. Laemmli, U. K. (1970) *Nature 227*, 680−685.
24. Cleveland, D. W., Fischer, S. G., Kirschner, M. W., and Laemmli, U. K. (1977) *J. Biol.* Chem. *252*, 1102−1106.
25. Blanton, M. P., Dangott, L. J., Raja, S. K., Lala, A. K., and Cohen, J. B. (1998) *J. Biol. Chem 273*, 8659−8668.
26. Pedersen, S. E., Dreyer, E. B., and Cohen, J. B. (1986) *J. Biol. Chem. 261*, 13735−13743.
27. Corbin, J., Methot, N., Wang, H. H., Baenziger, J. E., and Blanton, M. P. (1998) *J. Biol.* Chem. *273*, 771−777.

28. Carr, C., McCourt, D., and Cohen, J. B. (1987) *Biochemistry 26*, 7090−7102.
29. Blanton, M. P., Dangott, L. J., Xie, Y., and Cohen, J. B. (1997) *Biophys J. 72*, 152a.
30. Akabas, M. H. and Karlin, A. (1995) *Biochemistry 34*, 12496−12500.
31. Zhang, H., and Karlin, A. (1997) *Biochemistry 36*, 15856−15864.
32. Sigrist, H., Muhlemann, M., and Dolder, M. (1990) *J. Photochem. Photobiol. B 7*, 277−287.
33. Kim, J., and McNamee, M. G. (1998) *Biochemistry 37*, 4680−4686.
34. Tamamizu, S., Todd, A. P., and McNamee, M. G. (1995) *Cell. Mol. Neurobio. 15*, 427−438.

BI981435Q